Hard processes in p+Pb with Pythia/Angantyr: impact parameters and centrality biases

Oleh Fedkevych and Ilkka Helenius

Particle Physics Day 2026, Helsinki, November 11, 2026

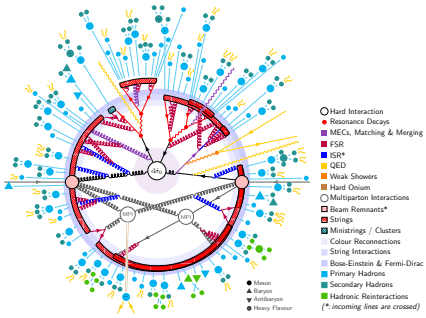


JYVÄSKYLÄN YLIOPISTO
UNIVERSITY OF JYVÄSKYLÄ



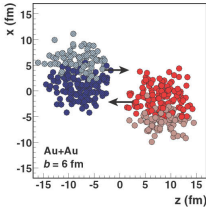
Centre of Excellence
in Quark Matter

Pythia and Angantyr



[pp → $t\bar{t}$ event in Pythia: Fig. 1 of the Pythia 8.3 manual, 2203.11601]





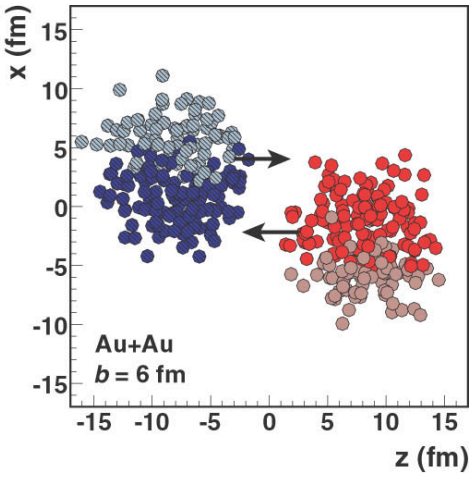
[A+A collision: nucl-ex/0701025]



[H. Hamilton, *Hjalmar friar till Ingeborg*]

Angantyr: arXiv:1806.10820

Heavy-ion collisions in Pythia: the Angantyr framework



[from arXiv:nucl-ex/0701025]

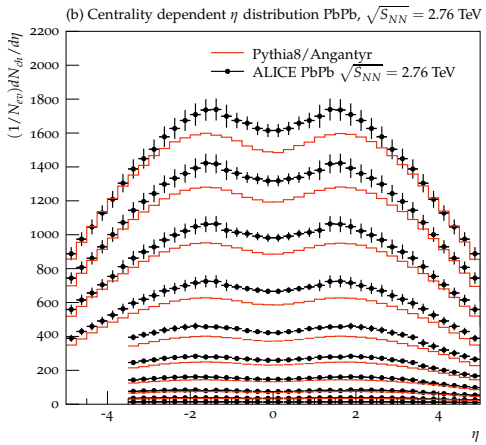
Angantyr model

- Introduced in 1806.10820; based on the Fritiof model Nucl. Phys. B281 (1987) 289 and on the concept of "wounded nucleons" Nucl. Phys. B111 (1976) 461
- Can be used as a baseline to understand collectivity

Main idea

- Set the collision geometry using Glauber MC
- Identify individual sub-collisions
- Determine the impact parameter of each pair
- Run Pythia pp machinery for each sub-collision
- Combine the events

Angantyr vs. ALICE Pb-Pb data

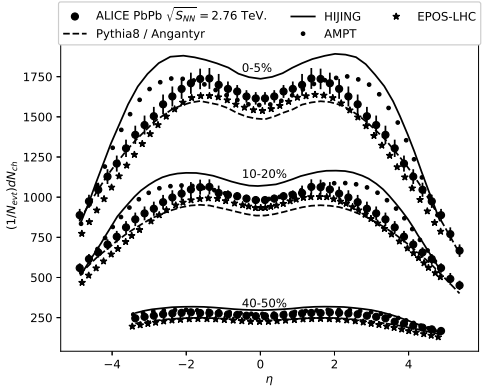


[Angantyr vs. ALICE Pb-Pb data, from 1806.10820]

Comparison with data

- Both HIJING and Angantyr are based on an "extrapolation" of pp dynamics to AA collisions.
- AMPT assumes that a hot, dense medium is formed (HIJING provides the initial conditions).
- EPOS is based on Gribov–Regge theory (no Glauber MC).
- AMPT gives too-wide distributions, HIJING overestimates the data, and Angantyr underestimates them; EPOS does better than Angantyr at mid-η but worse away from the central region.

Angantyr vs. ALICE Pb-Pb data

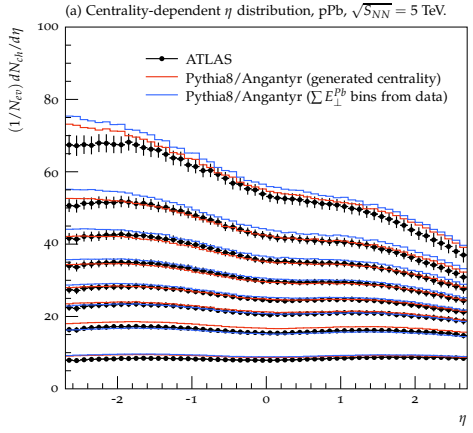


[EPOS-LHC, AMPT, HIJING and Angantyr vs. ALICE Pb-Pb data, from 1806.10820]

Comparison with data

- Both HIJING and Angantyr are based on an “extrapolation” of pp dynamics to AA collisions.
- AMPT assumes that a hot, dense medium is formed (HIJING provides the initial conditions).
- EPOS is based on Gribov–Regge theory (no Glauber MC).
- AMPT gives too-wide distributions, HIJING overestimates the data, and Angantyr underestimates them; EPOS does better than Angantyr at mid-η but worse away from the central region.

Angantyr vs. ATLAS pPb data

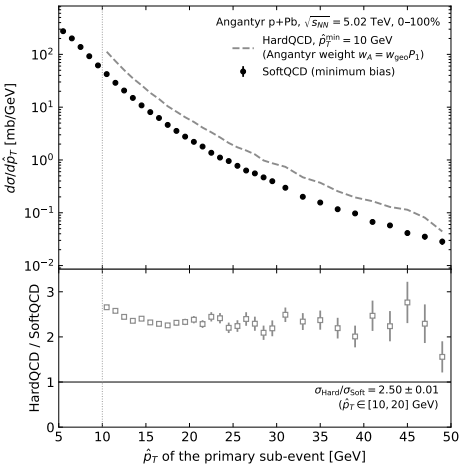


[Angantyr vs. ATLAS pPb data, from 1806.10820]

Comparison with data

- Unlike in the Pb-Pb case, Angantyr gives a fair description of the ATLAS pPb data (note that the ATLAS data are not unfolded).
- However, the charged-particle multiplicity distribution is mostly populated by MB events (SoftQCD mode in Pythia 8).
- Such events are abundant.
- But what if we want to study rare events with a large momentum transfer, e.g. the production of high-p_{T} jets in pA collisions?

SoftQCD vs. HardQCD in Angantyr: the $\hat{p}_T$ spectra



[Angantyr p+Pb, $\sqrt{s_{NN}} = 5.02$ TeV, 0–100%, original Angantyr weight]

Two samples, one cross section

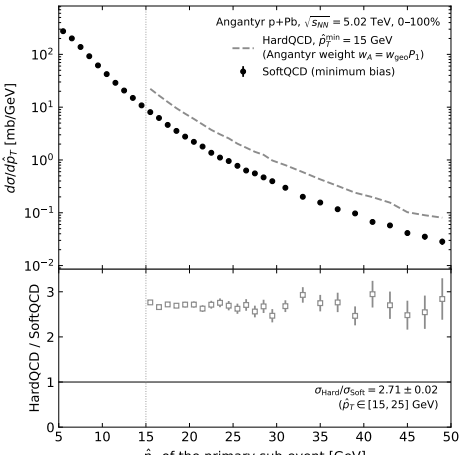
- **SoftQCD**: MC for **minimum-bias** events. Weight $w_{\rm geo}$.
- **HardQCD**: MC for **rare events** (jets): primary sub-collision is a $2 \to 2, \hat{p}_T > \hat{p}_T^{\min}$. Weight $w_A = w_{\rm geo} P_1$.

$w_{\rm geo} = \exp(b^2/2W^2), W = 8.89$ fm: undoes the Gaussian sampling of b.
$P_1 = 1 - (1 - w_1)^{N_{\rm abs}}, w_1 = \sigma_{\rm gen}^{\rm signal}/\sigma_{\rm ND}$: probability that ≥ 1 of the $N_{\rm abs}$ absorptive sub-collisions is hard.

Mismatch: HardQCD / SoftQCD above $\hat{p}_T^{\min}$

- $\hat{p}_T^{\min} = 10$ GeV: 2.50 ± 0.01, flat in $\hat{p}_T$.

SoftQCD vs. HardQCD in Angantyr: the $\hat{p}_T$ spectra



[Angantyr p+Pb, $\sqrt{s_{NN}} = 5.02$ TeV, 0–100%, original Angantyr weight]

Two samples, one cross section

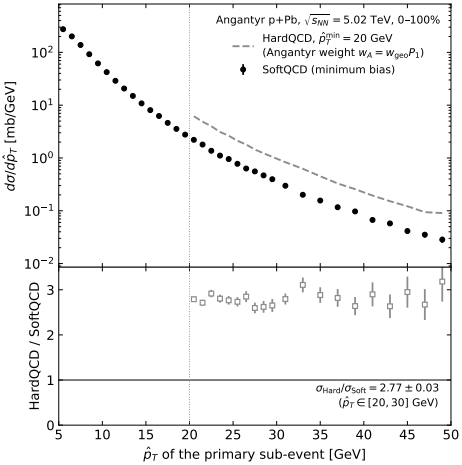
- **SoftQCD**: MC for **minimum-bias** events. Weight $w_{\rm geo}$.
- **HardQCD**: MC for **rare events** (jets): primary sub-collision is a $2 \to 2, \hat{p}_T > \hat{p}_T^{\min}$. Weight $w_A = w_{\rm geo} P_1$.

$w_{\rm geo} = \exp(b^2/2W^2), W = 8.89$ fm: undoes the Gaussian sampling of b.
$P_1 = 1 - (1 - w_1)^{N_{\rm abs}}, w_1 = \sigma_{\rm gen}^{\rm signal}/\sigma_{\rm ND}$: probability that ≥ 1 of the $N_{\rm abs}$ absorptive sub-collisions is hard.

Mismatch: HardQCD / SoftQCD above $\hat{p}_T^{\min}$

- $\hat{p}_T^{\min} = 10$ GeV: 2.50 ± 0.01, flat in $\hat{p}_T$.
- $\hat{p}_T^{\min} = 15$ GeV: 2.71 ± 0.02.

SoftQCD vs. HardQCD in Angantyr: the $\hat{p}_T$ spectra



[Angantyr p+Pb, $\sqrt{s_{NN}} = 5.02$ TeV, 0–100%, original Angantyr weight]

Two samples, one cross section

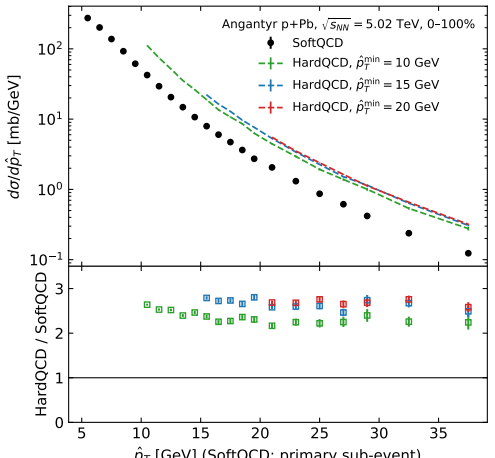
- **SoftQCD**: MC for **minimum-bias** events. Weight $w_{\rm geo}$.
- **HardQCD**: MC for **rare events** (jets): primary sub-collision is a $2 \to 2, \hat{p}_T > \hat{p}_T^{\min}$. Weight $w_A = w_{\rm geo} P_1$.

$w_{\rm geo} = \exp(b^2/2W^2), W = 8.89$ fm: undoes the Gaussian sampling of b.
$P_1 = 1 - (1 - w_1)^{N_{\rm abs}}, w_1 = \sigma_{\rm gen}^{\rm signal}/\sigma_{\rm ND}$: probability that ≥ 1 of the $N_{\rm abs}$ absorptive sub-collisions is hard.

Mismatch: HardQCD / SoftQCD above $\hat{p}_T^{\min}$

- $\hat{p}_T^{\min} = 10$ GeV: 2.50 ± 0.01, flat in $\hat{p}_T$.
- $\hat{p}_T^{\min} = 15$ GeV: 2.71 ± 0.02.
- $\hat{p}_T^{\min} = 20$ GeV: 2.77 ± 0.03.
- HardQCD too central: $\langle N_{\rm abs} \rangle = 9.2$–$10.5$ vs. 6.3.

SoftQCD vs. HardQCD in Angantyr: mismatch of the $\hat{p}_T$ spectra

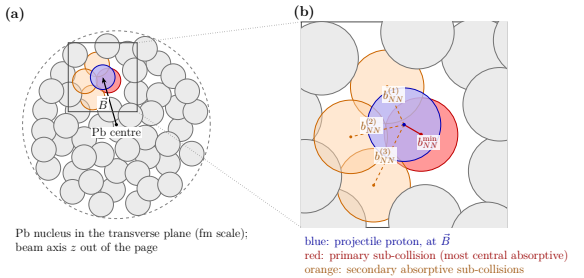


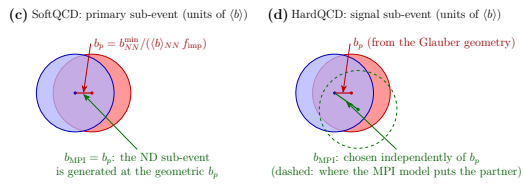
[Angantyr p+Pb, $\sqrt{s_{NN}} = 5.02$ TeV, 0–100%, original Angantyr weights]

SoftQCD and HardQCD do not match

- Primary absorptive sub-collision: SoftQCD $\rightarrow$ pp non-diffractive; HardQCD $\rightarrow 2 \rightarrow 2$ with $\hat{p}_T > \hat{p}_T^{\min}$. All other sub-collisions: minimum bias.
- HardQCD weight: $w_A = w_{\text{geo}} P_1$, $P_1 = 1 - (1 - w_1)^{N_{\text{abs}}}$, $w_1 = \sigma_{\text{gen}}^{\text{signal}} / \sigma_{\text{ND}}$ (at least one of N_{abs} sub-collisions is hard).
- Above the cut, HardQCD is 2.5–2.7$\times$ SoftQCD, for every $\hat{p}_T^{\min} = 10, 15, 20$ GeV.
- HardQCD events are more central: $\langle N_{\text{abs}} \rangle \approx 9$–$10.5$ vs. 6.3 in SoftQCD.
- Merging by event counts (jet-yield slides) removes the jump, not the centrality bias.

Collision geometry in Angantyr: the impact parameters





- (a) $\vec{B}$: p+Pb impact parameter. Sampled from a Gaussian of width W, compensated by the weight $w_{\text{geo}} = \exp(B^2/2W^2)$.
- (b) b_{NN} of every NN sub-collision: the absorptive one with the smallest b_{NN} is the primary, the others are secondary, $b_{NN}^{\min} < b_{NN}^{(1)} < b_{NN}^{(2)} < b_{NN}^{(3)}$.
- $b_p = b_{NN}^{\min}/(\langle b \rangle_{NN} f_{\text{imp}})$: the primary b_{NN} in Pythia units $\langle b \rangle$.
- (c) SoftQCD: the primary sub-event is generated at $b_{\text{MPI}} = b_p$, so its MPI activity follows the geometry.
- (d) HardQCD: a separate Pythia instance chooses b_{MPI} independently of b_p.

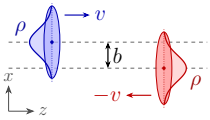
MPI model of Pythia and its connection to Angantyr

Master formula for the $2 \to 2$ cross section of the n^{th} interaction

$$\frac{d\sigma}{dp_\perp^2} = \sum_{j_1 j_2 j_3 j_4} \int dx_1\, dx_2\, d\hat{t}\, f_{j_1}(x_1, Q)\, f_{j_2}(x_2, Q)\, \frac{d\sigma_{j_1 j_2 \to j_3 j_4}}{d\hat{t}}\, \delta\left(p_\perp^2 - \frac{\hat{t}\hat{u}}{\hat{s}}\right)$$

The number of interactions is proportional to the overlap $\tilde{\mathcal{O}}(b)$

$$\tilde{\mathcal{O}}(b) = \int d^4x\, \rho_{\text{boosted}}\left(x - \frac{b}{2}, y, z - vt\right) \rho_{\text{boosted}}\left(x + \frac{b}{2}, y, z + vt\right)$$



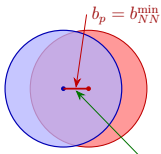
Geometry of pp collisions.

`bProfile=1`: $\mathcal{O}(b) \propto e^{-b^2}$

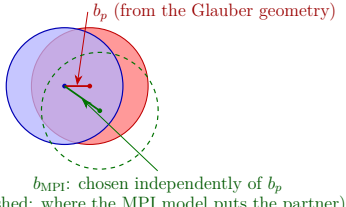
`bProfile=2`: $\mathcal{O}(b) \propto f_A e^{-b^2/R_A^2} + f_B e^{-b^2/R_B^2}$

`bProfile=3`: $\mathcal{O}(b) \propto e^{-b^p}$

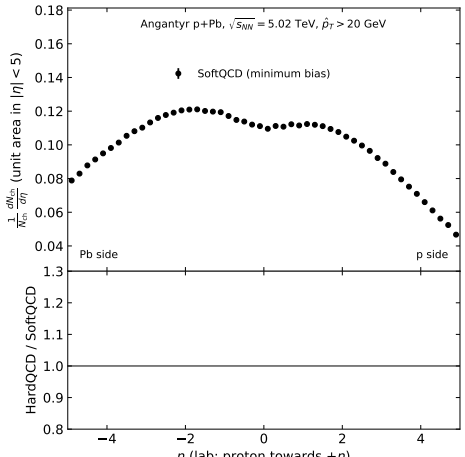
(c) SoftQCD: primary sub-event (units of $\langle b \rangle$)



(d) HardQCD: signal sub-event (units of $\langle b \rangle$)



SoftQCD vs. HardQCD in Angantyr: shape of $dN_{\mathrm{ch}}/d\eta$



[Angantyr p+Pb, $\sqrt{s_{NN}} = 5.02$ TeV, 0–100%, original Angantyr weight]

Observable

$\frac{1}{N_{\mathrm{ch}}} \frac{dN_{\mathrm{ch}}}{d\eta}$, $N_{\mathrm{ch}} = \int_{|\eta|<5} d\eta \, \frac{dN_{\mathrm{ch}}}{d\eta}$ (lab frame), events with primary $\hat{p}_T > 20$ GeV.

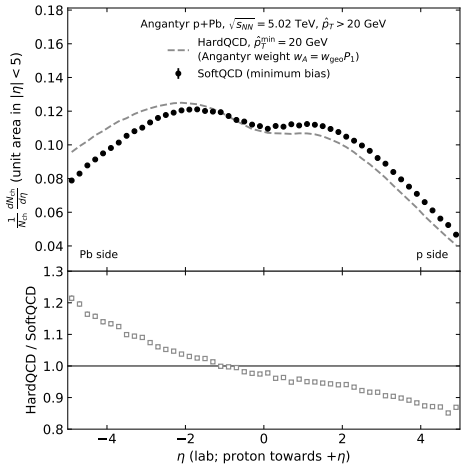
$w = w_{\mathrm{geo}}$ (SoftQCD), $w = w_{\mathrm{geo}} P_1$ (HardQCD),

$w_{\mathrm{geo}} = \exp(b^2/2W^2)$, $P_1 = 1 - (1 - w_1)^{N_{\mathrm{abs}}}$.

$dN_{\mathrm{ch}}/d\eta$ probes the MPI

N_{ch} and $dN_{\mathrm{ch}}/d\eta$ are sensitive to the MPI (Buckley et al., 1101.2599): the wrong N_{abs} and MPI activity of HardQCD show up directly in $dN_{\mathrm{ch}}/d\eta$.

SoftQCD vs. HardQCD in Angantyr: shape of $dN_{\rm ch}/d\eta$



[Angantyr p+Pb, $\sqrt{s_{NN}} = 5.02$ TeV, 0–100%, original Angantyr weight]

Observable

$\frac{1}{N_{\rm ch}}\frac{dN_{\rm ch}}{d\eta}, N_{\rm ch} = \int_{|\eta|<5} d\eta\, \frac{dN_{\rm ch}}{d\eta}$ (lab frame), events with primary $\hat{p}_T > 20$ GeV.

$w = w_{\rm geo}$ (SoftQCD), $w = w_{\rm geo}P_1$ (HardQCD),
$w_{\rm geo} = \exp(b^2/2W^2), P_1 = 1 - (1 - w_1)^{N_{\rm abs}}$.

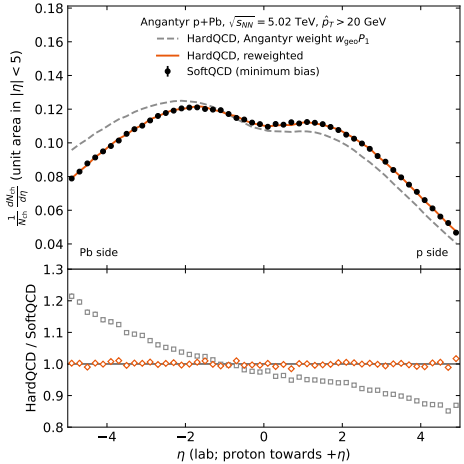
Problem

- HardQCD tilted to Pb: $+21\%$ at $\eta = -5$, -13% at $\eta = +5$.
- P_1 favours large $N_{\rm abs}$ (10.5 vs. 6.3): wrong underlying event.

$dN_{\rm ch}/d\eta$ probes the MPI

$N_{\rm ch}$ and $dN_{\rm ch}/d\eta$ are sensitive to the MPI (Buckley et al., 1101.2599): the wrong $N_{\rm abs}$ and MPI activity of HardQCD show up directly in $dN_{\rm ch}/d\eta$.

Reweighting HardQCD to SoftQCD: shape of $dN_{\mathrm{ch}}/d\eta$



[Angantyr p+Pb, $\sqrt{s_{NN}} = 5.02$ TeV, 0–100%, $\hat{p}_T^{\mathrm{min}} = 20$ GeV]

Weight of a HardQCD event

$$w = w_{\mathrm{geo}}(b)\, P(Q > Q_0 \mid b_p)\, \frac{K_s(b_{\mathrm{MPI}}, b_p)}{h(b_{\mathrm{MPI}})},$$

$$w_{\mathrm{geo}}(b) = \exp(b^2/2W^2), \quad W = 8.89\,\mathrm{fm},$$

$$K_s(b_{\mathrm{MPI}}, b_p) = G(b_{\mathrm{MPI}} - b_p) + G(b_{\mathrm{MPI}} + b_p),$$

$$G(x) = \frac{e^{-x^2/2s^2}}{\sqrt{2\pi}\, s}, \quad s = 0.1.$$

- $P(Q > Q_0 \mid b_p)$: fraction of SoftQCD events with primary $\hat{p}_T > Q_0$, in bins of b_p. Replaces P_1.
- $h(b_{\mathrm{MPI}}) = \frac{1}{N}\frac{dN}{db_{\mathrm{MPI}}}$: normalised distribution of b_{MPI} in HardQCD, $\int db_{\mathrm{MPI}}\, h = 1$ (unweighted, since b_{MPI} is independent of the geometry).

Result

Shape of $dN_{\mathrm{ch}}/d\eta$: $\chi^2 = 34/49$ (vanilla $9437/49$).
Cost: $N_{\mathrm{eff}}/N = 0.15$ (vanilla 0.55).

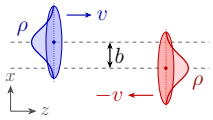
MPI model of Pythia and its connection to Angantyr

Master formula for the $2 \to 2$ cross section of the n^{th} interaction

$$\frac{d\sigma}{dp_\perp^2} = \sum_{j_1 j_2 j_3 j_4} \int dx_1\, dx_2\, d\hat{t}\, f_{j_1}(x_1, Q)\, f_{j_2}(x_2, Q)\, \frac{d\sigma_{j_1 j_2 \to j_3 j_4}}{d\hat{t}}\, \delta\left(p_\perp^2 - \frac{\hat{t}\hat{u}}{\hat{s}}\right)$$

The number of interactions is proportional to the overlap $\tilde{\mathcal{O}}(b)$

$$\tilde{\mathcal{O}}(b) = \int d^4x\, \rho_{\text{boosted}}\left(x - \frac{b}{2}, y, z - vt\right)\, \rho_{\text{boosted}}\left(x + \frac{b}{2}, y, z + vt\right)$$



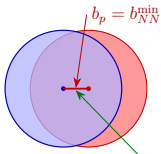
Geometry of pp collisions.

`bProfile=1`: $\mathcal{O}(b) \propto e^{-b^2}$

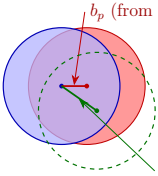
`bProfile=2`: $\mathcal{O}(b) \propto f_A e^{-b^2/R_A^2} + f_B e^{-b^2/R_B^2}$

`bProfile=3`: $\mathcal{O}(b) \propto e^{-b^p}$

(c) SoftQCD: primary sub-event (units of $\langle b \rangle$)



(d) HardQCD: signal sub-event (units of $\langle b \rangle$)



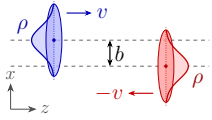
MPI model of Pythia and its connection to Angantyr

Master formula for the $2 \to 2$ cross section of the n^{th} interaction

$$\frac{d\sigma}{dp_\perp^2} = \sum_{j_1 j_2 j_3 j_4} \int dx_1\, dx_2\, d\hat{t}\, f_{j_1}(x_1, Q)\, f_{j_2}(x_2, Q)\, \frac{d\sigma_{j_1 j_2 \to j_3 j_4}}{d\hat{t}}\, \delta\left(p_\perp^2 - \frac{\hat{t}\hat{u}}{\hat{s}}\right)$$

The number of interactions is proportional to the overlap $\tilde{\mathcal{O}}(b)$

$$\tilde{\mathcal{O}}(b) = \int d^4x\, \rho_{\text{boosted}}\left(x - \frac{b}{2}, y, z - vt\right)\, \rho_{\text{boosted}}\left(x + \frac{b}{2}, y, z + vt\right)$$



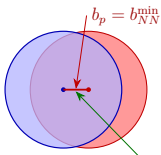
Geometry of pp collisions.

`bProfile=1`: $\mathcal{O}(b) \propto e^{-b^2}$

`bProfile=2`: $\mathcal{O}(b) \propto f_A e^{-b^2/R_A^2} + f_B e^{-b^2/R_B^2}$

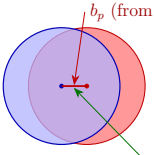
`bProfile=3`: $\mathcal{O}(b) \propto e^{-b^p}$

(c) SoftQCD: primary sub-event (units of $\langle b \rangle$)



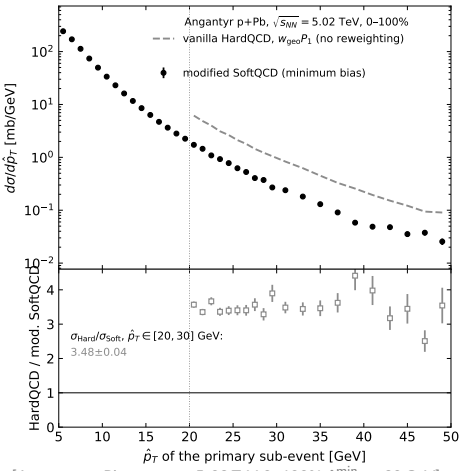
$b_{\text{MPI}} = b_p$: the ND sub-event is generated at the geometric b_p

(d) HardQCD: signal sub-event (units of $\langle b \rangle$)



$b_{\text{MPI}} = b_p$: the signal sub-event is generated at the geometric b_p

Modified Pythia ($b_{\mathrm{MPI}} = b_p$): the $\hat{p}_T$ spectrum



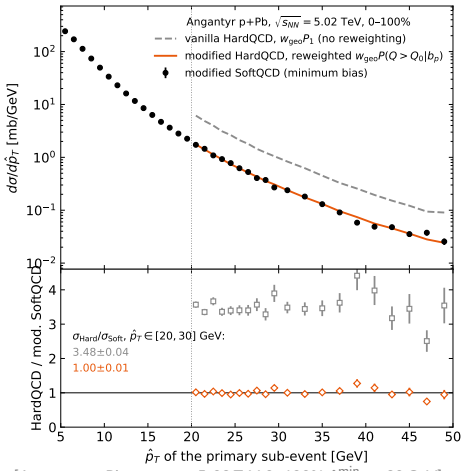
[Angantyr p+Pb, $\sqrt{s_{NN}} = 5.02$ TeV, 0–100%, $\hat{p}_T^{\mathrm{min}} = 20$ GeV]

Weight of a HardQCD event (modified Pythia)

$$w = w_{\mathrm{geo}}(b)\, P(Q > Q_0 \mid b_p),$$
$$w_{\mathrm{geo}}(b) = \exp(b^2/2W^2), \quad W = 8.89\ \mathrm{fm}.$$

- $P(Q > Q_0 \mid b_p)$: fraction of modified SoftQCD events with primary $\hat{p}_T > Q_0$, in bins of b_p. Replaces P_1.
- No K_s/h: the signal is already generated at $b_{\mathrm{MPI}} = b_p$.

Modified Pythia ($b_{\mathrm{MPI}} = b_p$): the $\hat{p}_T$ spectrum



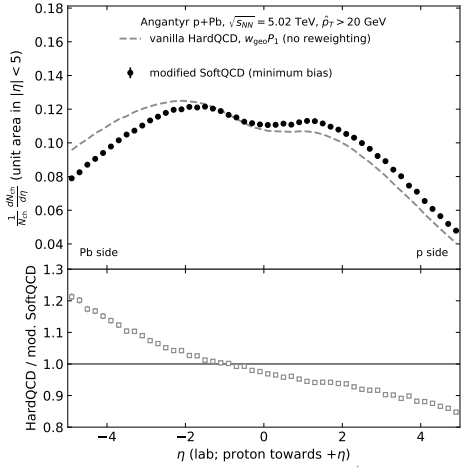
[Angantyr p+Pb, $\sqrt{s_{NN}} = 5.02$ TeV, 0–100%, $\hat{p}_T^{\mathrm{min}} = 20$ GeV]

Weight of a HardQCD event (modified Pythia)

$$w = w_{\mathrm{geo}}(b)\, P(Q > Q_0 \mid b_p),$$
$$w_{\mathrm{geo}}(b) = \exp(b^2/2W^2), \quad W = 8.89\ \mathrm{fm}.$$

- $P(Q > Q_0 \mid b_p)$: fraction of modified SoftQCD events with primary $\hat{p}_T > Q_0$, in bins of b_p. Replaces P_1.
- No K_s/h: the signal is already generated at $b_{\mathrm{MPI}} = b_p$.

Modified Pythia ($b_{\mathrm{MPI}} = b_p$): shape of $dN_{\mathrm{ch}}/d\eta$



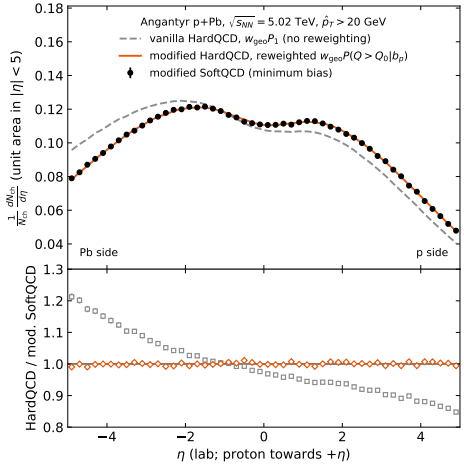
[Angantyr p+Pb, $\sqrt{s_{NN}} = 5.02$ TeV, 0–100%, $\hat{p}_T^{\mathrm{min}} = 20$ GeV]

Weight of a HardQCD event (modified Pythia)

$$w = w_{\mathrm{geo}}(b)\, P(Q > Q_0 \mid b_p),$$
$$w_{\mathrm{geo}}(b) = \exp(b^2/2W^2), \quad W = 8.89\,\mathrm{fm}.$$

- $P(Q > Q_0 \mid b_p)$: fraction of modified SoftQCD events with primary $\hat{p}_T > Q_0$, in bins of b_p. Replaces P_1.
- No K_s/h: the signal is already generated at $b_{\mathrm{MPI}} = b_p$.

Modified Pythia ($b_{\mathrm{MPI}} = b_p$): shape of $dN_{\mathrm{ch}}/d\eta$



[Angantyr p+Pb, $\sqrt{s_{NN}} = 5.02$ TeV, 0–100%, $\hat{p}_T^{\mathrm{min}} = 20$ GeV]

Weight of a HardQCD event (modified Pythia)

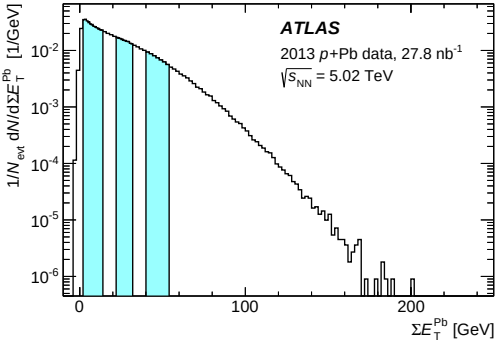
$$w = w_{\mathrm{geo}}(b)\, P(Q > Q_0 \mid b_p),$$
$$w_{\mathrm{geo}}(b) = \exp(b^2/2W^2), \quad W = 8.89\,\mathrm{fm}.$$

- $P(Q > Q_0 \mid b_p)$: fraction of modified SoftQCD events with primary $\hat{p}_T > Q_0$, in bins of b_p. Replaces P_1.
- No K_s/h: the signal is already generated at $b_{\mathrm{MPI}} = b_p$.

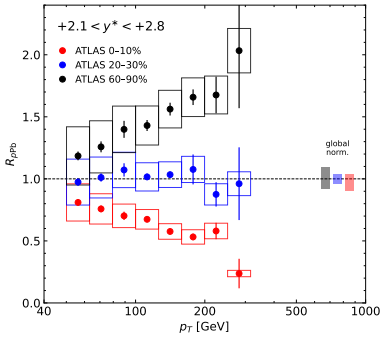
Result

Shape of $dN_{\mathrm{ch}}/d\eta$: $\chi^2 = 23/49$ (vanilla HardQCD, $w_{\mathrm{geo}}P_1$: 7482/49).
σ(HardQCD) / σ(SoftQCD) in [20, 30] GeV: 1.00.
Cost: $N_{\mathrm{eff}}/N = 0.74$ (vanilla Pythia with K_s/h: 0.15).

Centrality selection in p+Pb: ΣE_T^{Pb} in the forward calorimeter



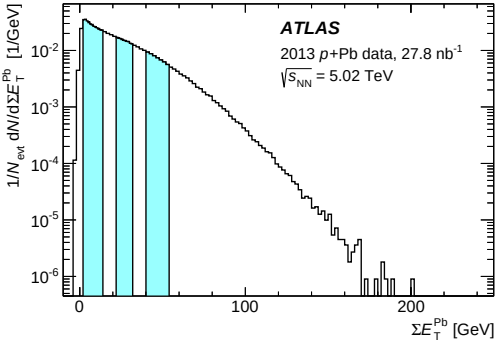
[ATLAS data, Fig. 1 of ATLAS: 1412.4092]



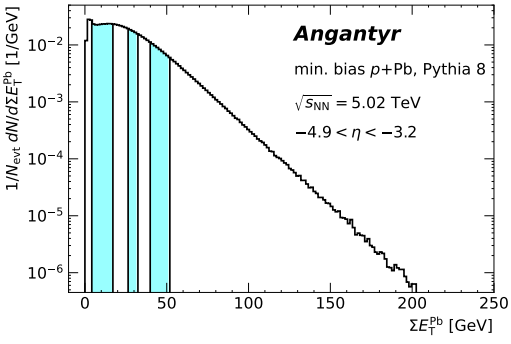
[ATLAS: 1412.4092]

- Centrality from ΣE_T^{Pb} in the FCal on the Pb-going side, $-4.9 < \eta < -3.2$: percentiles of the minimum-bias distribution. From right to left: 0–10%, 10–20%, 20–30%, 30–40%, 40–60%, 60–90%.

Centrality selection in p+Pb: ΣE_T^{Pb} in the forward calorimeter



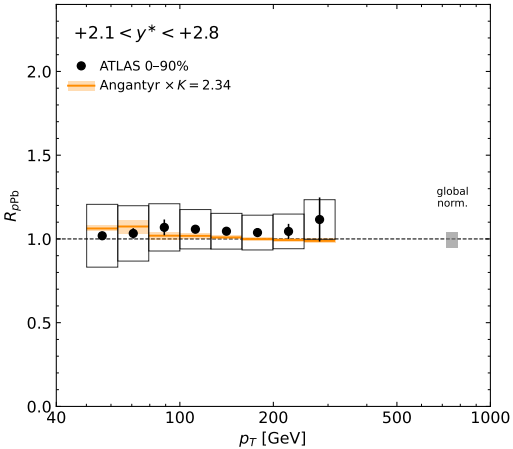
[ATLAS data, Fig. 1 of ATLAS: 1412.4092]



[Angantyr minimum-bias p+Pb, $\sqrt{s_{NN}} = 5.02$ TeV]

- Centrality from ΣE_T^{Pb} in the FCal on the Pb-going side, $-4.9 < \eta < -3.2$: percentiles of the minimum-bias distribution. From right to left: 0–10%, 10–20%, 20–30%, 30–40%, 40–60%, 60–90%.
- The same definition applied to Angantyr events (all final-state particles except neutrinos and muons): cuts at 51.9, 39.9, 32.4, 26.4, 17.1 and 4.2 GeV.

Kinematic biases in centrality selection: R_{pA} in 0–10%, 20–30%, 60–90% bins



[ATLAS: 1412.4092 vs. Angantyr]

$$R_{pA} = \frac{1}{\langle T_{pA} \rangle} \frac{(1/N_{\mathrm{evt}}) d^2N_{\mathrm{jet}}/dp_T\, dy^*|_{\mathrm{cent}}}{d^2\sigma^{pp}_{\mathrm{jet}}/dp_T\, dy^*},$$

$$\langle T_{pA} \rangle = \frac{\int_{c_1}^{c_2} d^2b\, T_{pA}(b)}{\int_{c_1}^{c_2} d^2b\, p_{\mathrm{inel}}(b)},$$

$$p_{\mathrm{inel}}(b) = 1 - \left(1 - \sigma^{NN}_{\mathrm{inel}} \frac{T_{pA}(b)}{A}\right)^A,$$

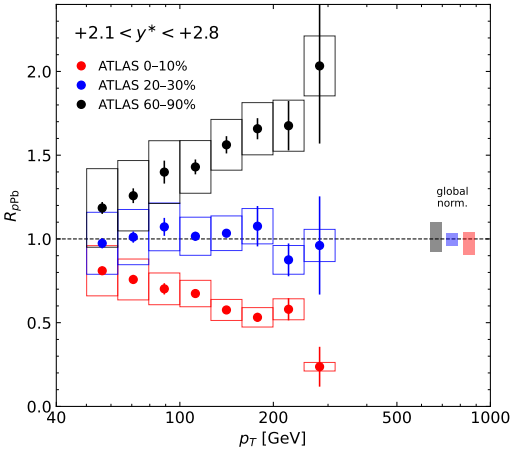
$$T_{pA}(b) = \int dz\, \rho_A(b,z),$$

$$y^* = \frac{1}{2} \log\left(\frac{E + p_z}{E - p_z}\right).$$

E, p_z in the NN c.m. frame.

MC: Angantyr (vanilla Pythia) $\times$ K, $K = 2.34 \pm 0.02$: one K for all y^* bins (0–90%).

Kinematic biases in centrality selection: R_{pA} in 0–10%, 20–30%, 60–90% bins



[ATLAS: 1412.4092]

$$R_{pA} = \frac{1}{\langle T_{pA} \rangle} \frac{(1/N_{\rm evt}) d^2 N_{\rm jet}/dp_T\, dy^*|_{\rm cent}}{d^2\sigma^{pp}_{\rm jet}/dp_T\, dy^*},$$

$$\langle T_{pA} \rangle = \frac{\int_{c_1}^{c_2} d^2b\, T_{pA}(b)}{\int_{c_1}^{c_2} d^2b\, p_{\rm inel}(b)},$$

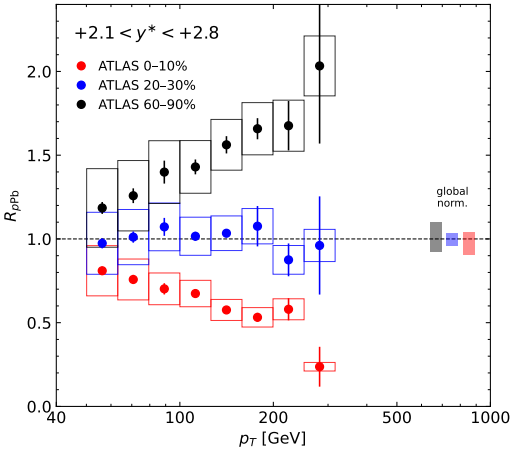
$$p_{\rm inel}(b) = 1 - \left(1 - \sigma^{NN}_{\rm inel} \frac{T_{pA}(b)}{A}\right)^A,$$

$$T_{pA}(b) = \int dz\, \rho_A(b,z),$$

$$y^* = \frac{1}{2} \log\left(\frac{E + p_z}{E - p_z}\right).$$

E, p_z in the NN c.m. frame.

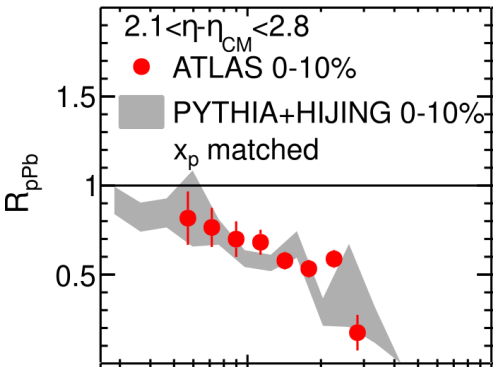
Kinematic biases in centrality selection: R_{pA} in 0–10%, 20–30%, 60–90% bins



[ATLAS: 1412.4092]

- Concept of centrality: the distribution of some final-state observable (e.g. transverse energy) is correlated with the collision impact parameter.
- Different definitions of centrality exist.
- Whereas centrality classification in non-peripheral AA collisions seems to be robust, the pA case is more problematic, see 1502.02986, 1304.3410 and 1412.8437.
- As pointed out in 1502.02986: "The usefulness of centrality selection relies, however, on how robustly it can be defined. Specifically [...] **whether there is a correlation between the characteristics of the events under consideration, say the requirement of presence of jets, and the centrality criterium**"

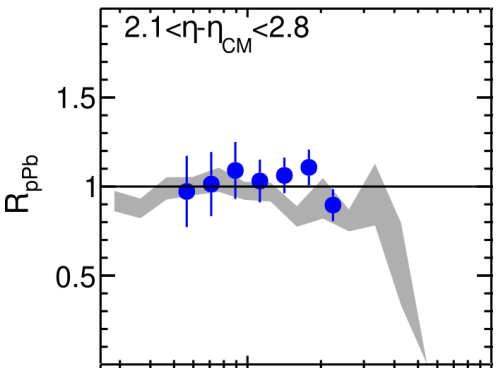
Kinematic biases: model of Armesto et al. 1502.02986



[from 1502.02986]

- Generate a pp event in Pythia without MPI.
- Extract the momentum fraction x_p of the hard parton.
- Generate an MB pA event in HIJING with $(1 - x_p)E_p$ and E_{Pb} beams, such that $\sqrt{s_{NN}} = 2\sqrt{(1 - x_p)E_p\, E_{\mathrm{Pb}}}$.
- Boost both events to the laboratory frame.
- Reweight the HIJING event such that the scaling with the number of collisions N_{coll} is preserved.
- Superimpose both events.
- The decreasing trend is captured.

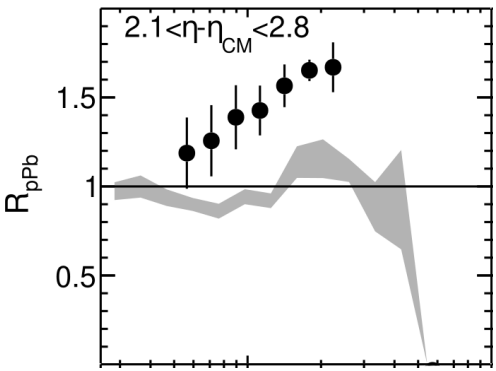
Kinematic biases: model of Armesto et al. 1502.02986



[from 1502.02986]

- Generate a pp event in Pythia without MPI.
- Extract the momentum fraction x_p of the hard parton.
- Generate an MB pA event in HIJING with $(1 - x_p)E_p$ and E_{Pb} beams, such that $\sqrt{s_{NN}} = 2\sqrt{(1 - x_p)E_p\, E_{\mathrm{Pb}}}$.
- Boost both events to the laboratory frame.
- Reweight the HIJING event such that the scaling with the number of collisions N_{coll} is preserved.
- Superimpose both events.
- The constant trend is captured.

Kinematic biases: model of Armesto et al. 1502.02986



[from 1502.02986]

- Generate a pp event in Pythia without MPI.
- Extract the momentum fraction x_p of the hard parton.
- Generate an MB pA event in HIJING with $(1 - x_p)E_p$ and E_{Pb} beams, such that $\sqrt{s_{NN}} = 2\sqrt{(1 - x_p)E_p\, E_{\mathrm{Pb}}}$.
- Boost both events to the laboratory frame.
- Reweight the HIJING event such that the scaling with the number of collisions N_{coll} is preserved.
- Superimpose both events.
- The increasing trend is not captured.

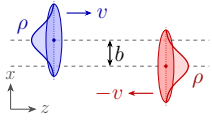
MPI model of Pythia and its connection to Angantyr

Master formula for the $2 \to 2$ cross section of the n^{th} interaction

$$\frac{d\sigma}{dp_\perp^2} = \sum_{j_1 j_2 j_3 j_4} \int dx_1\, dx_2\, d\hat{t}\, f_{j_1}(x_1, Q)\, f_{j_2}(x_2, Q)\, \frac{d\sigma_{j_1 j_2 \to j_3 j_4}}{d\hat{t}}\, \delta\left(p_\perp^2 - \frac{\hat{t}\hat{u}}{\hat{s}}\right)$$

The number of interactions is proportional to the overlap $\tilde{\mathcal{O}}(b)$

$$\tilde{\mathcal{O}}(b) = \int d^4x\, \rho_{\text{boosted}}\left(x - \frac{b}{2}, y, z - vt\right)\, \rho_{\text{boosted}}\left(x + \frac{b}{2}, y, z + vt\right)$$



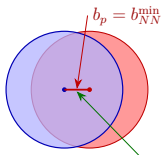
Geometry of pp collisions.

`bProfile=1`: $\mathcal{O}(b) \propto e^{-b^2}$

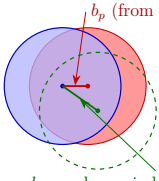
`bProfile=2`: $\mathcal{O}(b) \propto f_A e^{-b^2/R_A^2} + f_B e^{-b^2/R_B^2}$

`bProfile=3`: $\mathcal{O}(b) \propto e^{-b^p}$

(c) SoftQCD: primary sub-event (units of $\langle b \rangle$)



(d) HardQCD: signal sub-event (units of $\langle b \rangle$)



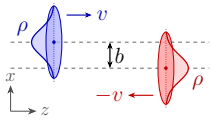
MPI model of Pythia and its connection to Angantyr

Master formula for the $2 \to 2$ cross section of the n^{th} interaction

$$\frac{d\sigma}{dp_\perp^2} = \sum_{j_1 j_2 j_3 j_4} \int dx_1\, dx_2\, d\hat{t}\, f_{j_1}(x_1, Q)\, f_{j_2}(x_2, Q)\, \frac{d\sigma_{j_1 j_2 \to j_3 j_4}}{d\hat{t}}\, \delta\left(p_\perp^2 - \frac{\hat{t}\hat{u}}{\hat{s}}\right)$$

The number of interactions is proportional to the overlap $\tilde{\mathcal{O}}(b)$

$$\tilde{\mathcal{O}}(b) = \int d^4x\, \rho_{\text{boosted}}\left(x - \frac{b}{2}, y, z - vt\right)\, \rho_{\text{boosted}}\left(x + \frac{b}{2}, y, z + vt\right)$$



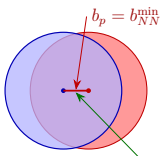
Geometry of pp collisions.

`bProfile=1`: $\mathcal{O}(b) \propto e^{-b^2}$

`bProfile=2`: $\mathcal{O}(b) \propto f_A e^{-b^2/R_A^2} + f_B e^{-b^2/R_B^2}$

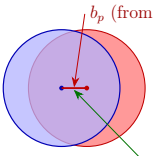
`bProfile=3`: $\mathcal{O}(b) \propto e^{-b^p}$

(c) SoftQCD: primary sub-event (units of $\langle b \rangle$)



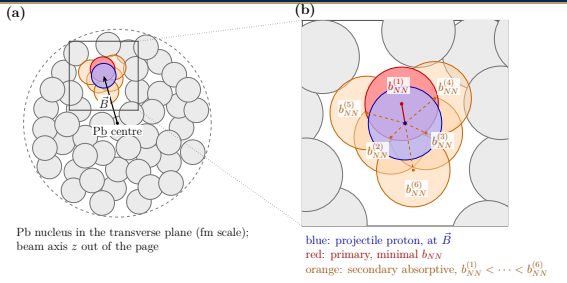
$b_{\text{MPI}} = b_p$: the ND sub-event is generated at the geometric b_p

(d) HardQCD: signal sub-event (units of $\langle b \rangle$)



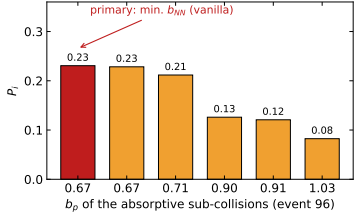
$b_{\text{MPI}} = b_p$: the signal sub-event is generated at the geometric b_p

Collision geometry in Angantyr: the impact parameters

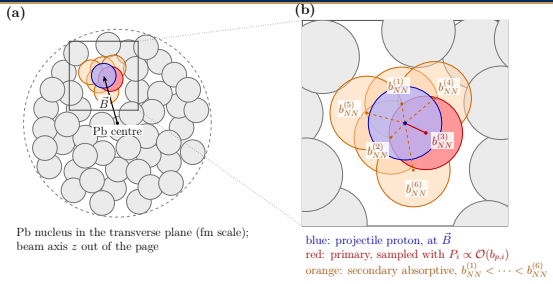


Which sub-collision is primary absorptive?

- Originally (vanilla Angantyr): the absorptive sub-collision with the minimal b_{NN}.
- New algorithm (modified Pythia):
  1) for each absorptive sub-collision i, convert $b_{NN,i}$ to $b_{p,i}$ and calculate $\mathcal{O}(b_{p,i})$;
  2) build the discrete distribution $P_i = \mathcal{O}(b_{p,i}) / \sum_j \mathcal{O}(b_{p,j})$, sample from it and decide which sub-collision is now the primary absorptive.

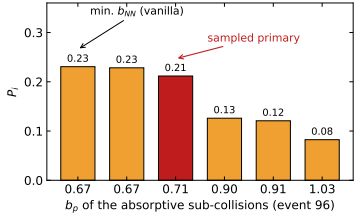


Collision geometry in Angantyr: the impact parameters

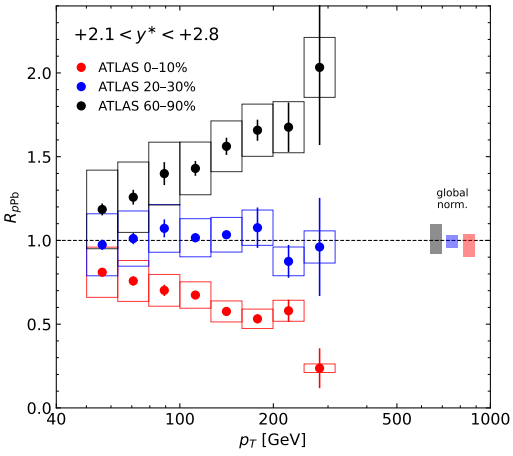


Which sub-collision is primary absorptive?

- Originally (vanilla Angantyr): the absorptive sub-collision with the minimal b_{NN}.
- New algorithm (modified Pythia):
  1) for each absorptive sub-collision i, convert $b_{NN,i}$ to $b_{p,i}$ and calculate $\mathcal{O}(b_{p,i})$;
  2) build the discrete distribution $P_i = \mathcal{O}(b_{p,i}) / \sum_j \mathcal{O}(b_{p,j})$, sample from it and decide which sub-collision is now the primary absorptive.



Kinematic biases in centrality selection: R_{pA} in 0–10%, 20–30%, 60–90% bins



[ATLAS: 1412.4092]

$$R_{pA} = \frac{1}{\langle T_{pA} \rangle} \frac{(1/N_{\rm evt}) d^2N_{\rm jet}/dp_T\, dy^*|_{\rm cent}}{d^2\sigma^{pp}_{\rm jet}/dp_T\, dy^*},$$

$$\langle T_{pA} \rangle = \frac{\int_{c_1}^{c_2} d^2b\, T_{pA}(b)}{\int_{c_1}^{c_2} d^2b\, p_{\rm inel}(b)},$$

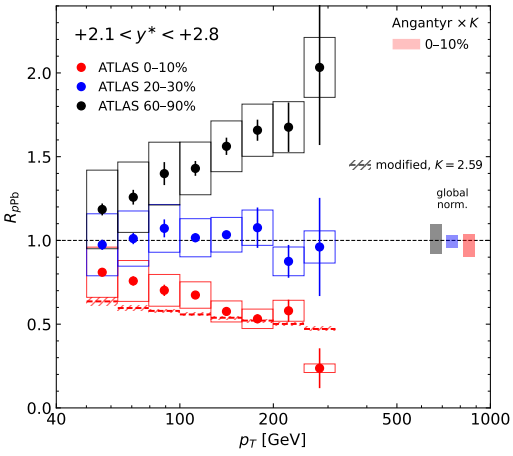
$$p_{\rm inel}(b) = 1 - \left(1 - \sigma^{NN}_{\rm inel} \frac{T_{pA}(b)}{A}\right)^A,$$

$$T_{pA}(b) = \int dz\, \rho_A(b,z),$$

$$y^* = \frac{1}{2} \log\left(\frac{E+p_z}{E-p_z}\right).$$

E, p_z in the NN c.m. frame.

Kinematic biases in centrality selection: R_{pA} in 0–10%, 20–30%, 60–90% bins



[ATLAS: 1412.4092 vs. Angantyr: modified Pythia]

$$R_{pA} = \frac{1}{\langle T_{pA} \rangle} \frac{(1/N_{\mathrm{evt}}) d^2N_{\mathrm{jet}}/dp_T\, dy^*|_{\mathrm{cent}}}{d^2\sigma^{pp}_{\mathrm{jet}}/dp_T\, dy^*},$$

$$\langle T_{pA} \rangle = \frac{\int_{c_1}^{c_2} d^2b\, T_{pA}(b)}{\int_{c_1}^{c_2} d^2b\, p_{\mathrm{inel}}(b)},$$

$$p_{\mathrm{inel}}(b) = 1 - \left(1 - \sigma^{NN}_{\mathrm{inel}} \frac{T_{pA}(b)}{A}\right)^A,$$

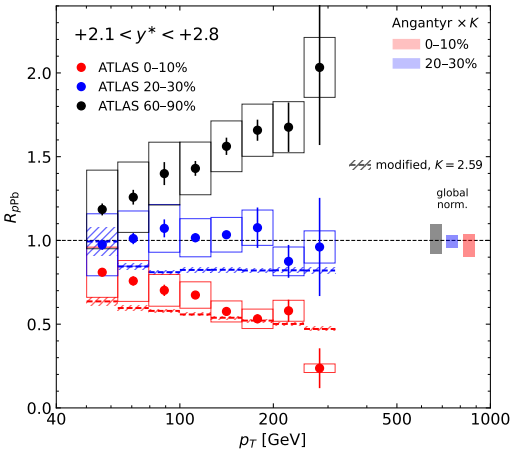
$$T_{pA}(b) = \int dz\, \rho_A(b,z),$$

$$y^* = \frac{1}{2} \log\left(\frac{E + p_z}{E - p_z}\right).$$

E, p_z in the NN c.m. frame.

MC: Angantyr × K, one K per Pythia version for all classes and y^* bins.

Kinematic biases in centrality selection: R_{pA} in 0–10%, 20–30%, 60–90% bins



[ATLAS: 1412.4092 vs. Angantyr: modified Pythia]

$$R_{pA} = \frac{1}{\langle T_{pA} \rangle} \frac{(1/N_{\rm evt}) d^2N_{\rm jet}/dp_T\, dy^*|_{\rm cent}}{d^2\sigma^{pp}_{\rm jet}/dp_T\, dy^*},$$

$$\langle T_{pA} \rangle = \frac{\int_{c_1}^{c_2} d^2b\, T_{pA}(b)}{\int_{c_1}^{c_2} d^2b\, p_{\rm inel}(b)},$$

$$p_{\rm inel}(b) = 1 - \left(1 - \sigma^{NN}_{\rm inel} \frac{T_{pA}(b)}{A}\right)^A,$$

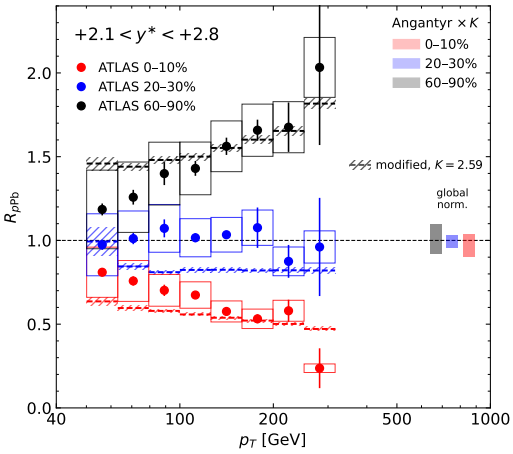
$$T_{pA}(b) = \int dz\, \rho_A(b,z),$$

$$y^* = \frac{1}{2} \log\left(\frac{E + p_z}{E - p_z}\right).$$

E, p_z in the NN c.m. frame.

MC: Angantyr × K, one K per Pythia version for all classes and y^* bins.

Kinematic biases in centrality selection: R_{pA} in 0–10%, 20–30%, 60–90% bins



[ATLAS: 1412.4092 vs. Angantyr: modified Pythia]

$$R_{pA} = \frac{1}{\langle T_{pA} \rangle} \frac{(1/N_{\mathrm{evt}}) d^2N_{\mathrm{jet}}/dp_T\, dy^*|_{\mathrm{cent}}}{d^2\sigma^{pp}_{\mathrm{jet}}/dp_T\, dy^*},$$

$$\langle T_{pA} \rangle = \frac{\int_{c_1}^{c_2} d^2b\, T_{pA}(b)}{\int_{c_1}^{c_2} d^2b\, p_{\mathrm{inel}}(b)},$$

$$p_{\mathrm{inel}}(b) = 1 - \left(1 - \sigma^{NN}_{\mathrm{inel}} \frac{T_{pA}(b)}{A}\right)^A,$$

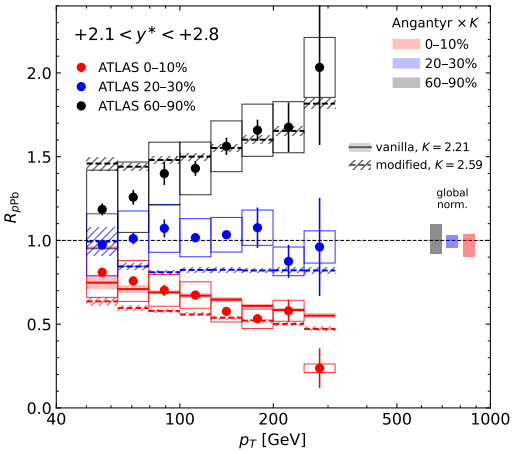
$$T_{pA}(b) = \int dz\, \rho_A(b,z),$$

$$y^* = \frac{1}{2} \log\left(\frac{E + p_z}{E - p_z}\right).$$

E, p_z in the NN c.m. frame.

MC: Angantyr × K, one K per Pythia version for all classes and y^* bins.

Kinematic biases in centrality selection: R_{pA} in 0–10%, 20–30%, 60–90% bins



[ATLAS: 1412.4092 vs. Angantyr: modified and vanilla Pythia]

$$R_{pA} = \frac{1}{\langle T_{pA} \rangle} \frac{(1/N_{\mathrm{evt}}) d^2N_{\mathrm{jet}}/dp_T\, dy^*|_{\mathrm{cent}}}{d^2\sigma^{pp}_{\mathrm{jet}}/dp_T\, dy^*},$$

$$\langle T_{pA} \rangle = \frac{\int_{c_1}^{c_2} d^2b\, T_{pA}(b)}{\int_{c_1}^{c_2} d^2b\, p_{\mathrm{inel}}(b)},$$

$$p_{\mathrm{inel}}(b) = 1 - \left(1 - \sigma^{NN}_{\mathrm{inel}} \frac{T_{pA}(b)}{A}\right)^A,$$

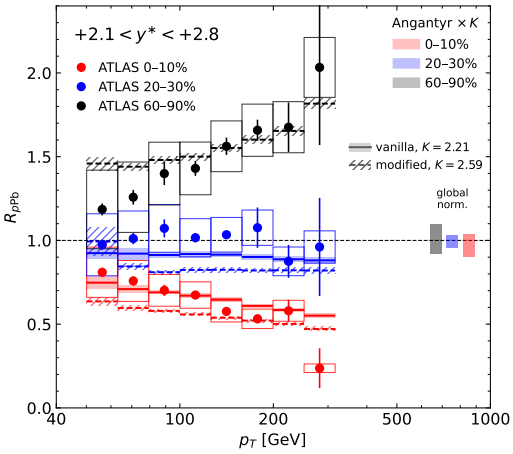
$$T_{pA}(b) = \int dz\, \rho_A(b,z),$$

$$y^* = \frac{1}{2} \log\left(\frac{E + p_z}{E - p_z}\right).$$

E, p_z in the NN c.m. frame.

MC: Angantyr × K, one K per Pythia version for all classes and y^* bins.

Kinematic biases in centrality selection: R_{pA} in 0–10%, 20–30%, 60–90% bins



[ATLAS: 1412.4092 vs. Angantyr: modified and vanilla Pythia]

$$R_{pA} = \frac{1}{\langle T_{pA} \rangle} \frac{(1/N_{\mathrm{evt}}) d^2N_{\mathrm{jet}}/dp_T\, dy^*|_{\mathrm{cent}}}{d^2\sigma^{pp}_{\mathrm{jet}}/dp_T\, dy^*},$$

$$\langle T_{pA} \rangle = \frac{\int_{c_1}^{c_2} d^2b\, T_{pA}(b)}{\int_{c_1}^{c_2} d^2b\, p_{\mathrm{inel}}(b)},$$

$$p_{\mathrm{inel}}(b) = 1 - \left(1 - \sigma^{NN}_{\mathrm{inel}} \frac{T_{pA}(b)}{A}\right)^A,$$

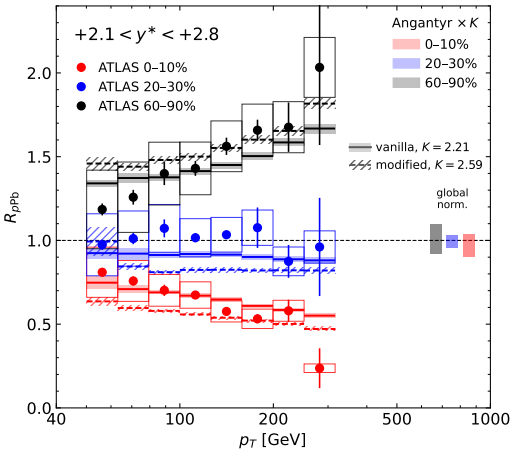
$$T_{pA}(b) = \int dz\, \rho_A(b, z),$$

$$y^* = \frac{1}{2} \log\left(\frac{E + p_z}{E - p_z}\right).$$

E, p_z in the NN c.m. frame.

MC: Angantyr × K, one K per Pythia version for all classes and y^* bins.

Kinematic biases in centrality selection: R_{pA} in 0–10%, 20–30%, 60–90% bins



[ATLAS: 1412.4092 vs. Angantyr: modified and vanilla Pythia]

$$R_{pA} = \frac{1}{\langle T_{pA} \rangle} \frac{(1/N_{\mathrm{evt}}) d^2N_{\mathrm{jet}}/dp_T\, dy^*|_{\mathrm{cent}}}{d^2\sigma^{pp}_{\mathrm{jet}}/dp_T\, dy^*},$$

$$\langle T_{pA} \rangle = \frac{\int_{c_1}^{c_2} d^2b\, T_{pA}(b)}{\int_{c_1}^{c_2} d^2b\, p_{\mathrm{inel}}(b)},$$

$$p_{\mathrm{inel}}(b) = 1 - \left(1 - \sigma^{NN}_{\mathrm{inel}} \frac{T_{pA}(b)}{A}\right)^A,$$

$$T_{pA}(b) = \int dz\, \rho_A(b, z),$$

$$y^* = \frac{1}{2} \log\left(\frac{E + p_z}{E - p_z}\right).$$

E, p_z in the NN c.m. frame.

MC: Angantyr × K, one K per Pythia version for all classes and y^* bins.

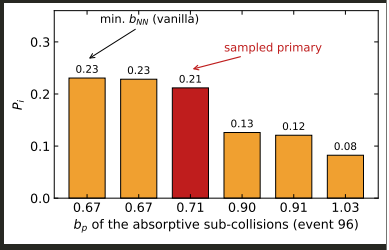
Conclusions

- There is currently a discontinuity between the SoftQCD and HardQCD modes of Pythia in p+A collisions.
- There is also a mismatch between the impact parameters from the Glauber MC and those of the Pythia MPI model.
- Both issues can be addressed by reweighting the HardQCD events.
- We fixed the impact-parameter mismatch ($b_{\mathrm{MPI}} = b_p$).
- We modified the way Angantyr selects the primary absorptive sub-collision: it is now chosen according to the matter overlap $\mathcal{O}(b_p)$.
- We qualitatively reproduce the trends of R_{pA}, but further improvements are needed (e.g. binary scaling is still broken).

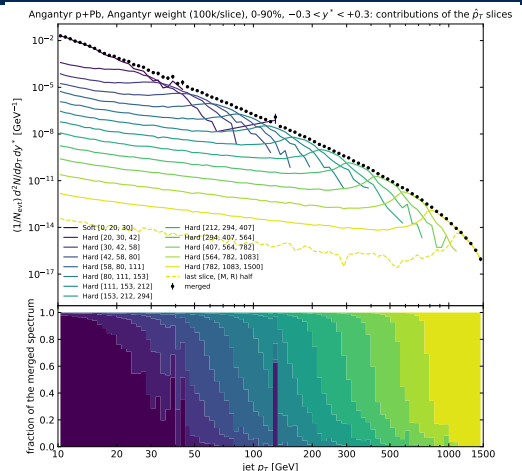
BACKUP SLIDES

Setting the primary absorptive interaction by sampling from $\mathcal{O}(b)$

```
iEvent = 96
 pick_sub_coll index = 0 bp = 6.70759e-01 calcOlap =  6.82186e-02
 pick_sub_coll index = 1 bp = 6.74978e-01 calcOlap =  6.75475e-02
 pick_sub_coll index = 2 bp = 7.06574e-01 calcOlap =  6.26234e-02
 pick_sub_coll index = 3 bp = 8.97299e-01 calcOlap =  3.72852e-02
 pick_sub_coll index = 5 bp = 9.11408e-01 calcOlap =  3.57338e-02
 pick_sub_coll index = 6 bp = 1.03088e+00 calcOlap =  2.43807e-02
 abs_pos = 0 olapp = 6.82186e-02
 abs_pos = 1 olapp = 6.75475e-02
 abs_pos = 2 olapp = 6.26234e-02
 abs_pos = 3 olapp = 3.72852e-02
 abs_pos = 5 olapp = 3.57338e-02
 abs_pos = 6 olapp = 2.43807e-02
 the primary absorptive is event # 2
 accepted event
```



Per-event jet yields in 0–90% p+Pb: merging of the $\hat{p}_T$ slices



[Angantyr p+Pb, $\sqrt{s_{NN}} = 5.02$ TeV, 10^5 events per $\hat{p}_T$ slice]

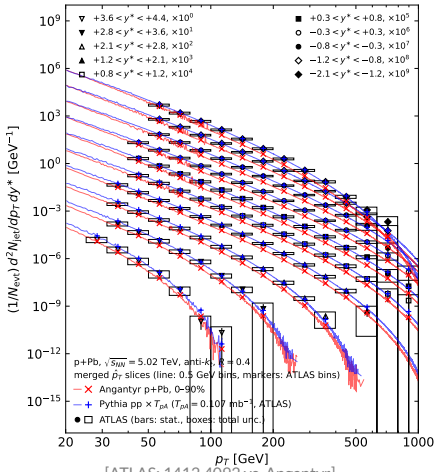
Merging of the $\hat{p}_T$ slices

Slice 0 is SoftQCD (Angantyr minimum bias), slices $i \geq 1$ are HardQCD, chained to it with the event counts N_L, N_R of the analysed centrality class c:

$$Y^c(p_T) = \frac{N^c_{L,0}}{N^c_{\mathrm{evt}}\,\Delta y^*} \sum_{i\geq 0} W^c_i \,\frac{h^c_i(p_T)}{N^c_{L,i}}, \qquad W^c_i = \prod_{j<i} \frac{N^c_{R,j}}{N^c_{L,j}},$$

- N^c_{evt}: all minimum-bias events of class c in the SoftQCD slice.
- $N^c_{L,i}, N^c_{R,i}$: events of class c in the lower / upper $\hat{p}_T$ half of slice i (the upper half of slice i is the lower half of slice $i+1$); h^c_i: jets from the lower half.
- pp reference: the same merging with $\sigma_{\mathrm{gen}}/\Sigma w$ of its SoftQCD slice, multiplied by T_{pA}.

Per-event jet yields in 0–90% p+Pb: Angantyr vs. ATLAS



[ATLAS: 1412.4092 vs. Angantyr]

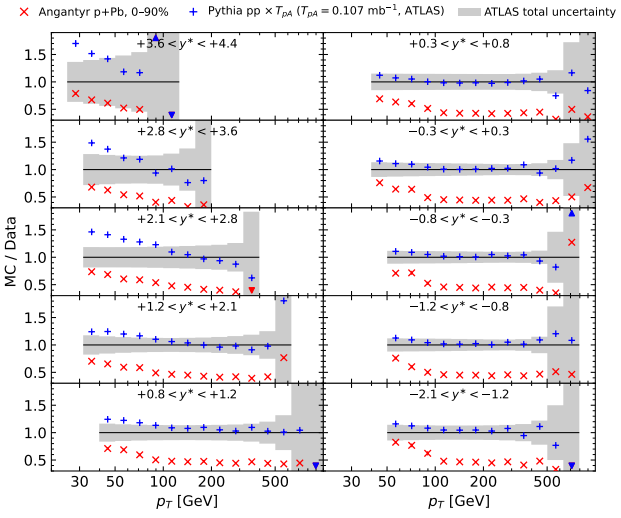
Merging of the $\hat{p}_T$ slices

Slice 0 is SoftQCD (Angantyr minimum bias), slices $i \geq 1$ are HardQCD, chained to it with the event counts N_L, N_R of the analysed centrality class c:

$$Y^c(p_T) = \frac{N^c_{L,0}}{N^c_{\text{evt}}\,\Delta y^*} \sum_{i\geq 0} W^c_i \,\frac{h^c_i(p_T)}{N^c_{L,i}}, \qquad W^c_i = \prod_{j<i} \frac{N^c_{R,j}}{N^c_{L,j}},$$

- N^c_{evt}: all minimum-bias events of class c in the SoftQCD slice.
- $N^c_{L,i}$, $N^c_{R,i}$: events of class c in the lower / upper $\hat{p}_T$ half of slice i (the upper half of slice i is the lower half of slice $i+1$); h^c_i: jets from the lower half.
- pp reference: the same merging with $\sigma_{\text{gen}}/\Sigma w$ of its SoftQCD slice, multiplied by T_{pA}.

Per-event jet yields in 0–90% p+Pb: MC/Data



[ATLAS: 1412.4092 vs. Angantyr]

Merging of the $\hat{p}_T$ slices

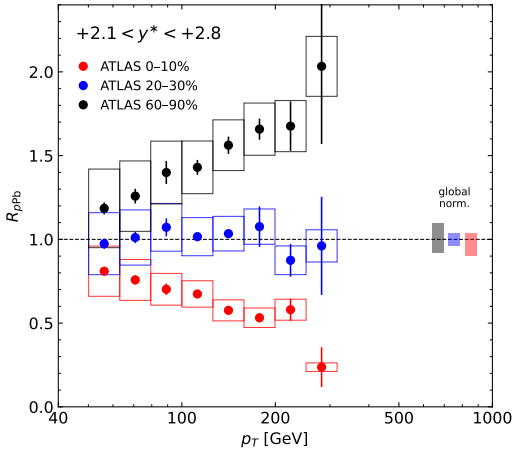
$$Y^c(p_T) = \frac{N^c_{L,0}}{N^c_{\mathrm{evt}}\,\Delta y^*} \sum_{i\geq 0} W^c_i \frac{h^c_i(p_T)}{N^c_{L,i}},$$

$$W^c_i = \prod_{j<i} \frac{N^c_{R,j}}{N^c_{L,j}},$$

$$T_{pA}\frac{d^2\sigma_{pp}}{dp_T\,dy^*} = T_{pA}\frac{N_{L,0}\,\sigma_{\mathrm{gen}}}{\Sigma w\,\Delta y^*} \sum_{i\geq 0} W_i \frac{h_i(p_T)}{N_{L,i}}.$$

- MC errors: histogram statistics ⊕ statistics of the slice weights W_i.
- Grey band: ATLAS total uncertainty.

Kinematic biases in centrality selection: R_{pA} in 0–10%, 20–30%, 60–90% bins



[ATLAS: 1412.4092]

$$R_{pA} = \frac{1}{\langle T_{pA} \rangle} \frac{(1/N_{\rm evt}) d^2N_{\rm jet}/dp_T\, dy^*|_{\rm cent}}{d^2\sigma^{pp}_{\rm jet}/dp_T\, dy^*},$$

$$\langle T_{pA} \rangle = \frac{\int_{c_1}^{c_2} d^2b\, T_{pA}(b)}{\int_{c_1}^{c_2} d^2b\, p_{\rm inel}(b)},$$

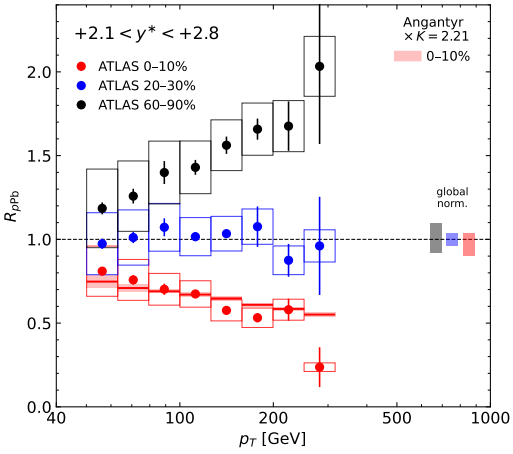
$$p_{\rm inel}(b) = 1 - \left(1 - \sigma^{NN}_{\rm inel} \frac{T_{pA}(b)}{A}\right)^A,$$

$$T_{pA}(b) = \int dz\, \rho_A(b,z),$$

$$y^* = \frac{1}{2} \log\left(\frac{E+p_z}{E-p_z}\right).$$

E, p_z in the NN c.m. frame.

Kinematic biases in centrality selection: R_{pA} in 0–10%, 20–30%, 60–90% bins



[ATLAS: 1412.4092 vs. Angantyr]

$$R_{pA} = \frac{1}{\langle T_{pA} \rangle} \frac{(1/N_{\mathrm{evt}}) d^2N_{\mathrm{jet}}/dp_T\, dy^*|_{\mathrm{cent}}}{d^2\sigma^{pp}_{\mathrm{jet}}/dp_T\, dy^*},$$

$$\langle T_{pA} \rangle = \frac{\int_{c_1}^{c_2} d^2b\, T_{pA}(b)}{\int_{c_1}^{c_2} d^2b\, p_{\mathrm{inel}}(b)},$$

$$p_{\mathrm{inel}}(b) = 1 - \left(1 - \sigma^{NN}_{\mathrm{inel}} \frac{T_{pA}(b)}{A}\right)^A,$$

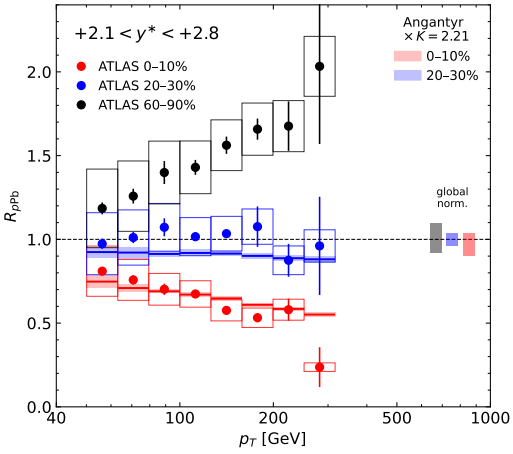
$$T_{pA}(b) = \int dz\, \rho_A(b,z),$$

$$y^* = \frac{1}{2} \log\left(\frac{E + p_z}{E - p_z}\right).$$

E, p_z in the NN c.m. frame.

MC: Angantyr (vanilla Pythia) $\times K$, $K = 2.21 \pm 0.02$: one K for all three classes and all y^* bins.

Kinematic biases in centrality selection: R_{pA} in 0–10%, 20–30%, 60–90% bins



[ATLAS: 1412.4092 vs. Angantyr]

$$R_{pA} = \frac{1}{\langle T_{pA} \rangle} \frac{(1/N_{\rm evt}) d^2N_{\rm jet}/dp_T\, dy^*|_{\rm cent}}{d^2\sigma^{pp}_{\rm jet}/dp_T\, dy^*},$$

$$\langle T_{pA} \rangle = \frac{\int_{c_1}^{c_2} d^2b\, T_{pA}(b)}{\int_{c_1}^{c_2} d^2b\, p_{\rm inel}(b)},$$

$$p_{\rm inel}(b) = 1 - \left(1 - \sigma^{NN}_{\rm inel} \frac{T_{pA}(b)}{A}\right)^A,$$

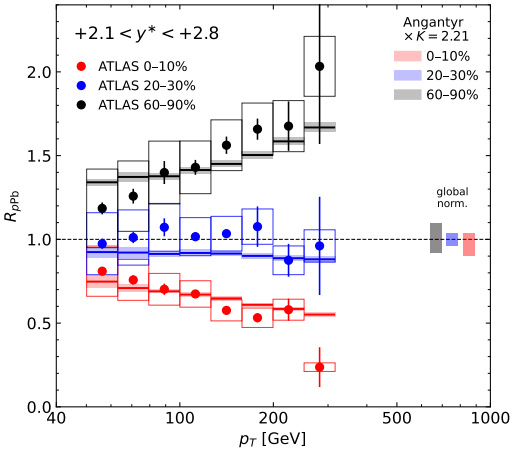
$$T_{pA}(b) = \int dz\, \rho_A(b,z),$$

$$y^* = \frac{1}{2} \log\left(\frac{E + p_z}{E - p_z}\right).$$

E, p_z in the NN c.m. frame.

MC: Angantyr (vanilla Pythia) $\times K$, $K = 2.21 \pm 0.02$: one K for all three classes and all y^* bins.

Kinematic biases in centrality selection: R_{pA} in 0–10%, 20–30%, 60–90% bins



[ATLAS: 1412.4092 vs. Angantyr]

$$R_{pA} = \frac{1}{\langle T_{pA} \rangle} \frac{(1/N_{\rm evt}) d^2N_{\rm jet}/dp_T\, dy^*|_{\rm cent}}{d^2\sigma^{pp}_{\rm jet}/dp_T\, dy^*},$$

$$\langle T_{pA} \rangle = \frac{\int_{c_1}^{c_2} d^2b\, T_{pA}(b)}{\int_{c_1}^{c_2} d^2b\, p_{\rm inel}(b)},$$

$$p_{\rm inel}(b) = 1 - \left(1 - \sigma^{NN}_{\rm inel} \frac{T_{pA}(b)}{A}\right)^A,$$

$$T_{pA}(b) = \int dz\, \rho_A(b,z),$$

$$y^* = \frac{1}{2} \log\left(\frac{E + p_z}{E - p_z}\right).$$

E, p_z in the NN c.m. frame.

MC: Angantyr (vanilla Pythia) $\times K$, $K = 2.21 \pm 0.02$: one K for all three classes and all y^* bins.